Proceedings of the 21st ICSMGE, Vienna, Austria, 14 – 19 June 2026. Pistrol, Adam & Schweiger (eds.)
Published by: ÖGG, Austrian Society for Geomechanics, Salzburg, Austria, ISBN 978-3-9503898-4-5
https://doi.org/10.53243/ICSMGE2026-2383

Fundamental Study on Seismic Behavior of Offshore Wind Energy Monopile Foundation with Seismic Damper

Yasuo Sawamura, Kouki Isobe
Department of Urban Management, Kyoto University, Japan, sawamura.yasuo.6c@kyoto-u.ac.jp

Toshiyasu Miyoshi, Makoto Yoshida
Offshore Wind Construction Business Divisions Group, Penta-Ocean Construction co., ltd., Japan

ABSTRACT: Offshore wind energy development is rapidly accelerating worldwide. In Japan, seismic safety is a critical concern due to frequent earthquakes. This study proposes a composite system in which seismic dampers are installed between a monopile foundation and an adjacent pier structure to reduce seismic response by utilizing phase differences. A series of three-dimensional elasto-plastic finite element analyses were performed to evaluate the effects of seismic dampers installation height and damping properties. The seismic dampers were modeled as a nonlinear, velocity-dependent dashpot. Comparisons with equivalent spring cases revealed that seismic dampers effectively reduced displacement of the monopile. Notably, the seismic dampers exhibited superior energy dissipation due to a slightly advanced resistance phase compared to spring elements. Under second-mode excitation, deformations resembling third-mode behavior were observed, resulting in significant changes in the distribution of bending moments. These findings confirm that the integrated seismic damper system improves seismic resilience in offshore monopile foundations and offers a viable vibration control strategy for earthquake-prone regions.

KEYWORDS: Offshore wind, Monopile foundation, Seismic damper, Finite element analysis, Vibration control.

1 INTRODUCTION

In recent years, the global expansion of offshore wind energy has accelerated significantly. In Japan, however, introducing offshore wind systems necessitates the assurance of seismic safety due to its tectonic activity. Among fixed-type offshore foundations, monopile structures are widely used due to their constructability and cost efficiency. Nonetheless, their dynamic behavior during seismic events remains a critical issue. To address this, the authors propose a composite structural system in which seismic dampers are installed between the monopile foundation and a surrounding pier structure (Figure 1). This composite structure is intended to reduce the seismic response of a monopile-type wind turbine during an earthquake. In this composite system, the seismic dampers are expected to exert a horizontal force by utilizing the phase difference between the monopile foundation and the pier structure during an earthquake.

In this study, a series of three-dimensional elasto-plastic finite element analyses were conducted to clarify the influence of the seismic dampers' installation position and damping characteristics on the seismic behavior of the system.

2 NUMERICAL ANALYSIS

2.1 *Model Overview*

The numerical analysis was conducted using the three-dimensional elasto-plastic finite element code DBLEAVES (Ye et al., 2007). The analysis aimed to investigate the fundamental seismic behavior of the composite structural system, based on centrifuge model experiments conducted by the authors (Isobe et al., 2023), with seismic dampers installed at various heights. Figure 2 illustrates the analytical mesh and boundary conditions.

The mechanical properties of the ground (Toyoura sand, relative density of 85%) were modeled using the subloading t_{ij} constitutive model (Nakai and Hinokio, 2004). Table 1 presents the parameters for Toyoura sand. The monopile and tower components were modeled using elastic beam elements. The beam elements of the monopile section were represented by a hybrid model (Kimura and Zhang, 2000), combining a high-stiffness beam element (90% stiffness) and a low-stiffness column elements (10% stiffness) to account for volume and

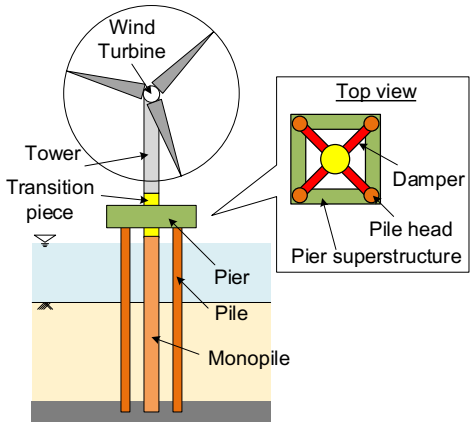

Figure 1. Schematic diagram of offshore wind energy monopile foundation with seismic dampers.

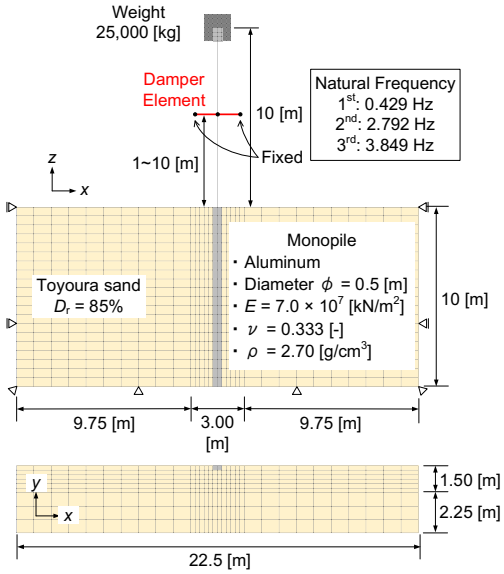

Figure 2. Analysis mesh and boundary conditions.

Table 1. Parameters for Toyoura sand.

Principal stress ratio at critical state $R_{cs} = (\sigma_1/\sigma_3)_{CS(comp.)}$	3.2
Compression index λ	0.07
Swelling index κ	0.0045
$N = e_{NC}$ at p = 98 kPa & q = 0 kPa	1.1
Poisson's ratio ν	0.271
Shape of yield surface β	2.0
Influence of density and confining pressure a	60

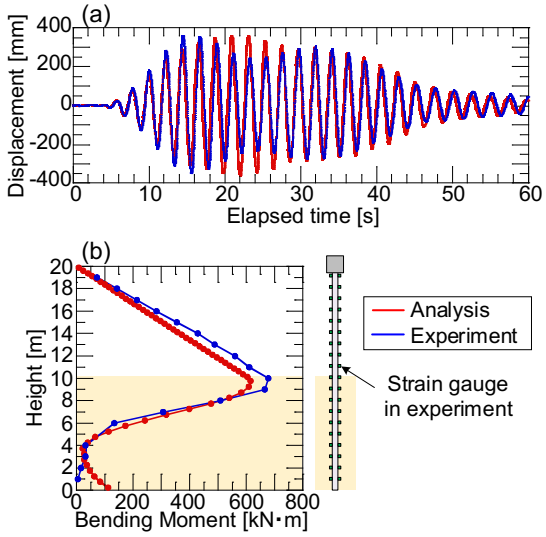

Figure 3. Results of centrifuge model experiment and reproduction analysis: (a) Displacement time history of tower top, (b) Distribution of maximum bending moments.

flexibility. Figure 3 shows an example of a reproduced analysis in which a 0.46 Hz sinusoidal wave with a maximum acceleration of approximately 1.0 m/s² was applied in a centrifuge model experiment. The figure demonstrates that the analytical model successfully replicates the experimental results with high accuracy.

2.2 *Analytical Conditions*

The purpose of this study is to investigate the basic characteristics of monopile foundations equipped with seismic dampers. As shown in Figure 2, seismic dampers were installed between the fixed points in the global coordinate system and the monopile without considering the pier structure. The installation positions of the seismic dampers were varied in 1-meter increments from z = 11 m (1 m above the ground surface) to z = 20 m (the installation position of the wind turbine), resulting in a total of 10 cases. Seismic dampers were modeled as viscous dampers (nonlinear dashpots) based on the research by Yunoki et al. (2009), where the resistance force is expressed as $F = CV^n$, where F is the resistance force [kN], C is the viscous coefficient [kN/(m/s)$^{0.3}$],V is velocity [m/s], n is velocity-dependence parameter [-]. The velocity-dependence parameter n was set to 0.3. The viscous coefficient C is determined based on the results of centrifuge model experiments, where the weight of the wind turbine was 25 tons, the maximum input acceleration was 1 m/s^2, and the maximum top velocity was approximately 1 m/s. Based on the value (25 tons × 1 m/s^2) / (1.0 m/s)$^{0.3}$ = 25 kN/(m/s)$^{0.3}$, three cases were examined: C = 10, 25, and 50 kN/(m/s)$^{0.3}$.

Furthermore, to compare the behavior with that of seismic dampers, the cases where springs were installed instead of seismic dampers were also examined. When setting the spring constant k [kN/m], the results of centrifuge model experiments were also referenced, where the weight of the wind turbine was

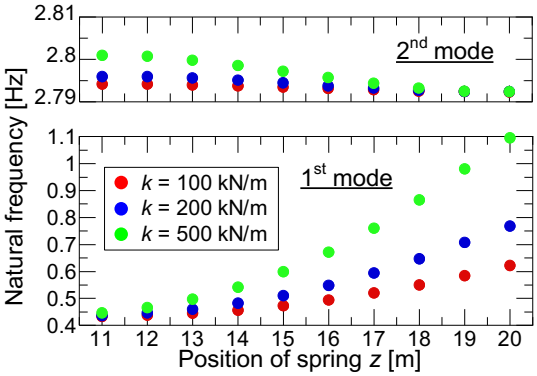

Figure 4. Relationship between the spring installation height and natural frequency of composite structural system.

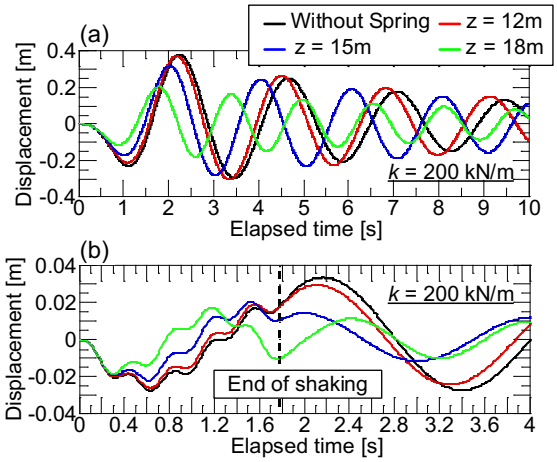

Figure 5. Displacement time history of tower top when springs are installed: (a) Input 0.5 Hz, (b) Input 2.80 Hz.

25 tons, the maximum input acceleration was 1 m/s², and a maximum top displacement was approximately 0.4 m. Thus, three cases were selected: k = 100, 200, and 500 kN/m.

The input seismic motions consisted of sinusoidal waves with an amplitude of 1 m/s². Three types of pulse waves were selected based on the first-order natural frequency of the monopile model (0.429 Hz): 0.25 Hz (smaller than the first-order natural frequency), 0.50 Hz (close to the first-order natural frequency), and 1.00 Hz (larger than the first-order natural frequency). Additionally, an input frequency of 2.80 Hz (5 waves) was selected as a representative of the second-order natural frequency, resulting in a total of four input motions.

3 RESULTS AND DISCUSSION

3.1 *Case with Spring*

Figure 4 shows the relationship between the spring installation height and the natural frequency of the composite structural system. The first-order natural frequency increases with spring height due to significant deformation at the tower top. Although spring stiffness affects frequency, the trend with height remains consistent. In contrast, the second-order natural frequency increases as the spring is installed lower due to central deformation dominance.

Figure 5 shows the displacement time history of the tower top for a spring constant k = 200 kN/m. From the results at an input frequency of 0.5 Hz in Figure 5(a), it can be confirmed that the displacement of the tower top is suppressed as the spring installation height increases. This trend is also observed at an input frequency of 0.25 Hz, 1.00 Hz, and higher spring constants result in smaller displacements under all input seismic

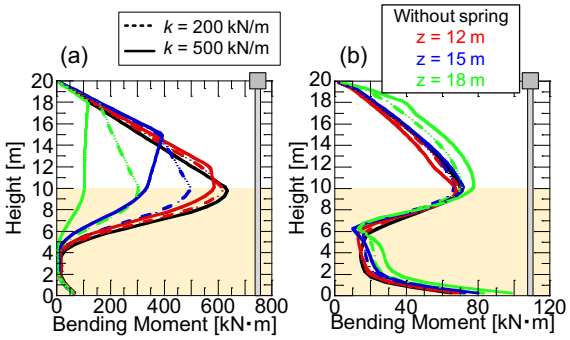

Figure 6. Maximum bending moment distribution of monopile and tower when springs are installed: (a) Input 0.5 Hz, (b) Input 2.80 Hz.

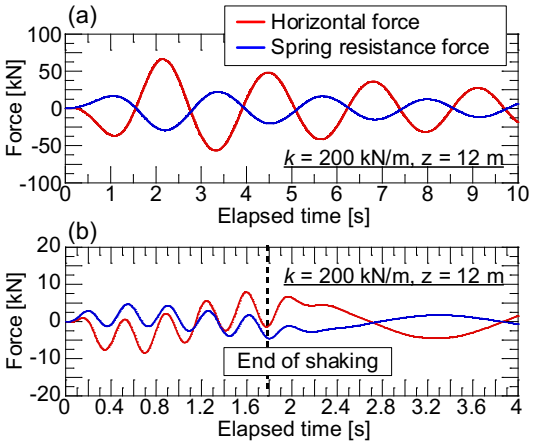

Figure 7. Time history of horizontal force at tower top and spring resistance force.: (a) Input 0.5 Hz, (b) Input 2.80 Hz.

motions. At an input frequency of 2.80 Hz, as shown in Figure 5(b), the monopile foundation and tower vibrates significantly at a frequency close to the first-order natural frequency during excitation, followed by fine vibrations near the input frequency of 2.80 Hz. By installing springs, the amplitude at frequencies near the first-order natural frequency decreases, but behavior of high-frequency vibrations near the input frequency of 2.80 Hz remains largely unchanged.

Figure 6 shows the distribution of the maximum bending moments occurring in the monopile and tower. For inputs near the first-order natural frequency, installing springs reduces the maximum bending moment in all cases. However, when focusing on the positions where springs were installed, the bending moment was larger in some cases compared to the case without springs. This is considered to be due to the significant effect of the resistance force exerted by the springs on the monopile and tower (hereinafter referred to as spring resistance force) against the vibrations of the monopile. On the other hand, when an input of 2.80 Hz near the second-order natural frequency was applied, there was little change in the bending moment at installation positions between 12 m and 15 m, but the bending moment increased at installation position 18 m. This is because installing a spring at 18 m amplified the deformation near the ground surface, thereby increasing the bending moment generated in the monopile and tower.

Figure 7 shows the time history of the horizontal force at the tower top (calculated by multiplying the acceleration at the tower top by the mass of the wind turbine hereinafter referred to as the top horizontal force) and the spring resistance force. At an input frequency of 0.50 Hz, the top horizontal force and the spring resistance force were in antiphase. This is because the maximum acceleration at the tower top occurs when the displacement is maximum, which coincides with the time when

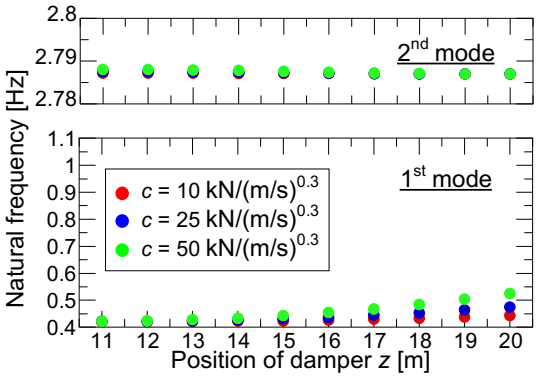

Figure 8. Relationship between the damper installation height and natural frequency of composite structural system.

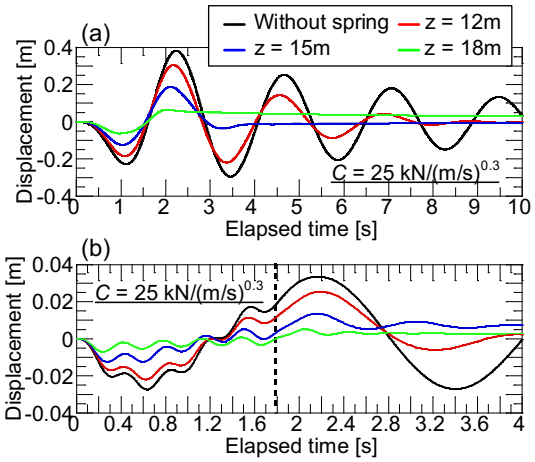

Figure 9. Displacement time history of tower top when seismic dampers are installed: (a) Input 0.5 Hz, (b) Input 2.80 Hz.

the spring resistance force reaches its maximum. On the other hand, when the input frequency is 2.80 Hz, the spring resistance force and the top horizontal force exhibit approximately the same phase. This indicates that directions of displacement at the tower top and the spring attachment point are reversed, resulting in deformation due to the second-order vibration mode.

3.2 *Case with Damper*

Figure 8 shows the relationship between the installation position of the seismic dampers and their natural frequencies. Both in first- and second-order natural frequencies, the trend is same as in the case of springs. However, in damped vibration systems, a damped natural frequency is defined separately from the system's natural frequency. The natural frequencies shown here are calculated solely through numerical analysis and may not necessarily match the system's natural frequency or damping natural frequency. This point should be noted.

Figure 9 shows the displacement time history of the tower top at a viscous coefficient C = 25 kN/(m/s)$^{0.3}$. As shown in Figure 9(a), near the first-order natural frequency, the displacement during excitation decreased in all cases with the seismic dampers installed. Additionally, after excitation ceased, vibration decayed more rapidly compared to the case without seismic dampers. In some cases, overdamped behavior was observed, where residual displacement occurs after the excitation ended. On the other hand, in the case of an input frequency of 2.80 Hz shown in Figure 9(b), installing seismic dampers reduced the amplitude of the large trend of vibrations near the first-order natural frequency, similar to when springs

were installed. However, the fine vibration behavior near the input frequency of 2.80 Hz remained largely unchanged.

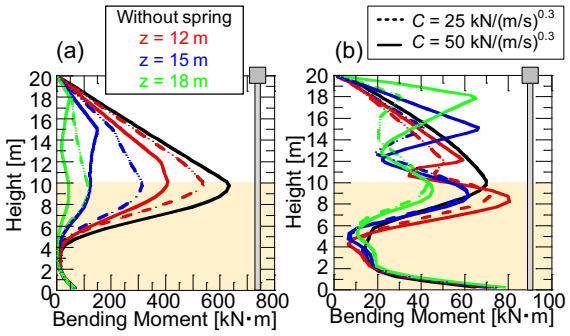

Figure 10. Maximum bending moment distribution of monopile and tower when seismic dampers are installed: (a) Input 0.5 Hz, (b) Input 2.80 Hz.

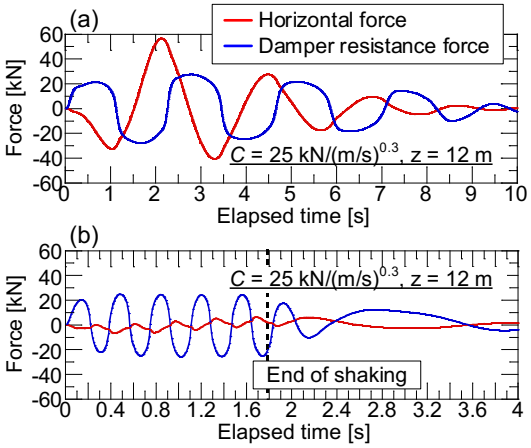

Figure 11. Time history of horizontal force at wind turbine and damper resistance force: (a) Input 0.5 Hz, (b) Input 2.80 Hz.

Figure 10 shows the distribution of the maximum bending moments occurring in the monopile and tower. For seismic motions near the first-order natural frequency, the bending moments at the locations where springs were installed were sometimes larger. However, when seismic dampers were installed, the bending moments in the tower section were smaller than those in the case without seismic dampers for all input frequencies. On the other hand, at an input frequency of 2.80 Hz, installing seismic dampers caused a significant change in the distribution shape of the bending moment distribution. At this time, the monopile and tower exhibited deformation resembling a third-order vibration mode, and it was confirmed that there were areas where the bending moments decreased and increased compared to the case without seismic dampers.

Figure 11 shows the time history of the top horizontal force and the resistance force (hereinafter referred to as damper resistance force) exerted by the seismic dampers on the monopile. Focusing on the case of an input frequency of 0.50 Hz, when springs were installed, the top horizontal force and the spring resistance force were in antiphase, but when seismic dampers were installed, the phase of the seismic damper resistance force was slightly ahead of the antiphase of the top horizontal force. This suggests that seismic dampers generate damping forces earlier than springs, thereby reducing monopile vibrations. On the other hand, at an input frequency of 2.80 Hz, when springs were installed, the top horizontal force and spring resistance force were in nearly the same phase, but when a seismic dampers were installed, it was confirmed that the phase of the seismic dampers resistance force were slightly ahead of the phase of the top horizontal force. From this, it is considered that while it is difficult to suppress deformation caused by the second vibration mode using springs, installing seismic dampers makes it possible to suppress deformation caused by the second vibration mode.

4 CONCLUSIONS

In this study, three-dimensional elasto-plastic finite element analysis was used to investigate the fundamental changes in the dynamic characteristics of monopile foundations equipped with either springs or seismic dampers. The key findings are summarized as follows:

(1) Installing springs or seismic dampers at higher locations increases the first-order natural frequency; placing them near mid-height enhances second mode response.

(2) Seismic dampers provide superior vibration control due to phase-advanced resistance forces.

(3) Seismic dampers effectively reduce deformation in both first and second vibrational modes and suppress bending moments more evenly than springs.

(4) At higher input frequencies, complex mode shapes resembling third-mode behavior were observed, especially with seismic damper installation.

(5) The results demonstrate the effectiveness of seismic dampers for offshore monopile foundations and suggest a promising strategy for improving resilience in seismic zones.

These findings may contribute to the future development of seismic design guidelines for offshore wind energy infrastructure in seismically active regions

5 REFERENCES

Isobe, K., Sawamura, Y., Miyoshi, T., Yoshida, M. and Bai, K. 2023. Fundamental Experiment on Seismic Behavior of Offshore Wind Turbine Monopile Foundation with Integrated Damper. *Proc. of the 58th Japan National Conference on Geotechnical Engineering*, Fukuoka, 11-9-1-06. (in Japanese)

Kimura, M. and Zhang, F. 2000. Seismic Evaluations of Pile Foundations with Three Different Methods Based on Three Dimensional Elasto-plastic Finite Element Analysis. *Soils and Foundations*, 40(5), 113-132.

Nakai, T. and Hinokio, M. 2004. A simple elastoplastic model for normally and over consolidated soils with unified material parameters. *Soils and Foundations*, 44(2), 53-70..

Ye, B., Ye, G. L., Zhang, F. and Yashima, A. 2007. Experiment and numerical simulation of repeated liquefaction-consolidation of sand. *Soils and Foundations*, 47(3), 547-558.

Yunoki, K., Mazda, T., Uno, H. and Miyamoto, H. 2009. Response evaluation of highway bridge considering varied types of modeling for structural control damper. *JSCE Journal of Earthquake Engineering*, 65(1), 378-387. (in Japanese)